arXiv:1207.1770v1 [cond-mat.str-el] 7 Jul 2012

Correlation Assisted Phonon Softenings and the Mott-Peierls Transition in VO_2

Sooran Kim, Kyoo Kim, Chang-Jong Kang, and B. I. Min
Department of physics, PCTP, Pohang University of Science and Technology, Pohang, 790-784, Korea

To explore the driving mechanisms of the metal-insulator transition (MIT) and the structural transition in VO_2, we have investigated phonon dispersions of rutile VO_2 (R-VO_2) in the DFT and the DFT+U (U: Coulomb correlation) band calculations. We have found that the phonon softening instabilities occur in both cases, but the softened phonon mode only in the DFT+U describes properly both the MIT and the structural transition from R-VO_2 to monoclinic VO_2 (M_1-VO_2). This feature demonstrates that the Coulomb correlation effect plays an essential role of assisting the Peierls transition in R-VO_2. We have also found from the phonon dispersion of M_1-VO_2 that M_1 structure becomes unstable under high pressure. We have predicted a new phase of VO_2 at high pressure that has a monoclinic $CaCl_2$-type structure with metallic nature.

PACS numbers: 63.20.dk, 63.20.D-, 71.30.+h, 71.10.Fd

Vanadium dioxide (VO_2) is one of the most explored transition metal oxides due to its intriguing metal-insulator transition (MIT) and the concomitant structural transition upon cooling. At ambient pressure and high temperature, VO_2 has a tetragonal rutile-type structure (R-VO_2) with metallic nature. Upon cooling below 340 K, R-VO_2 undergoes the structural transition to a monoclinic structure (M_1-VO_2) with insulating nature.[1, 2] The mechanism of MIT in VO_2 has been a longstanding subject of controversy. In the structural transition from R-VO_2 to M_1-VO_2, V ions construct the dimerization and the zigzag distortion. In R-VO_2, V ions are centered at the distorted O_6 octahedra, which are edge-shared along the c-axis. Due to the crystal field, V $3d$ states are split into a_{1g} ($d_{\parallel}$), e_g^{π} (π^*), and e_g^{σ} states in order of energy, and so one electron of V^{4+} ion occupies the lowest a_{1g} state. While the zigzag distortion increases the energy of e_g^{π} bands, the dimerization of V-V causes the splitting of a_{1g} bands to open the gap at the Fermi level (E_F).[3] This kind of structural distortion is explained by a typical Peierls transition.

However, the density functional theory (DFT) band approach fails to describe the insulating nature of M_1-VO_2 properly.[3–5] The energy gap at E_F can be obtained only when the extra Coulomb correlation U effect of V $3d$ electrons is considered, which indicates that M_1-VO_2 is a Mott-Hubbard type insulator. Hence the Mott-Hubbard transition was proposed as the mechanism of MIT in VO_2.[6–8] Beyond the DFT band approach, the GW[9–11] or the hybrid functional band method[12] was employed to describe the insulating nature of M_1-VO_2 properly. There were also the DMFT (dynamical mean-field theory) approaches to explain the insulating nature of M_1-VO_2 by considering the Mott-Hubbard U explicitly.[5, 13–15] Therefore the consensus at the moment is that some amount of U is necessary to describe the insulating nature of M_1-VO_2.[16, 17] However, whether R-VO_2 is a strongly correlated system or whether U is necessary for the MIT has not been clarified yet, despite a few existing studies using the DFT+U[18, 19] and the DMFT.[5, 14, 20]

Besides R-VO_2 and M_1-VO_2, other structural types of VO_2 were reported, such as monoclinic M_2-VO_2, M_3-VO_2 and triclinic T-VO_2, which are stabilized under the uniaxial stress or with doping of Cr or Al.[21–25] All the monoclinic phases of M_1, M_2, and M_3-VO_2 are insulators at ambient pressure, but at the pressure above 10 GPa, M_1-VO_2, Cr-doped M_2-VO_2, and Cr-doped M_3-VO_2 become metallic with some type of monoclinic structure, so called, M_x phase.[26–28] Still the real structure of M_x phase has not been identified yet.

As described above, there have been extensive electronic structure studies on VO_2. By contrast, there have been only several phonon studies on VO_2.[29–31, 33, 36] Especially, there has been neither experimental nor theoretical report on the phonon dispersion curve for VO_2 yet. Since the Peierls transition is closely related to the phonon softening instability, the study of phonon dispersions of VO_2 is expected to give a clue to understanding the mechanism of MIT in VO_2.[32–36]

In this letter, we have revisited the MIT and the structural transition of VO_2 by investigating the phonon dispersions of R-VO_2 and M_1-VO_2. We have found that R-VO_2 is a strongly correlated system with $U \geq 4.0$ eV, and the Coulomb correlation effect plays an essential role in the structural transition from R-VO_2 to M_1-VO_2. We have also studied the structural stability of M_1-VO_2 under pressure, and found that M_1 phase becomes unstable to a phase that seems to be related to M_x phase.

We consider the two phase of VO_2, R-VO_2 and M_1-VO_2, the space groups of which correspond to $P4_2/mnm$ and $P2_1/c$, respectively.[3] For the electronic structure and phonon dispersion calculations, the pseudo-potential band method and the supercell approach that are implemented in VASP[37] and PHONOPY[38] are used. The utilized exchange-correlation functional is the generalized gradient approximation (GGA). The adopted values of U and J in the DFT+U are 4.2 eV and 0.8 eV, respectively.[5] All the phonon calculations were done after the full relaxation of the volume and atomic

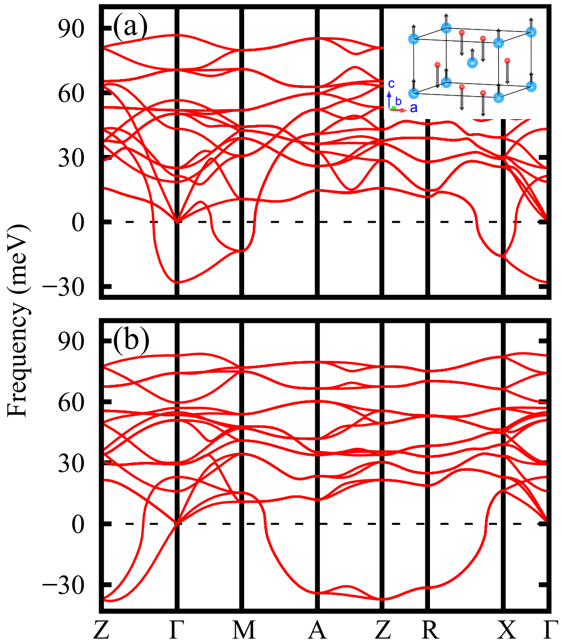

FIG. 1: (Color online) (a) The phonon dispersion curves of R-VO$_2$ in the DFT. The inset figure shows the normal mode of softened phonon at Γ. (b) The phonon dispersion curves of R-VO$_2$ in the DFT+U. Both figures show the negative phonon frequencies (imaginary frequencies) corresponding to the phonon softening instability.

positions.[39] The initial structural parameters of R-VO$_2$ and M_1-VO$_2$ before the relaxation are taken from McWhan *et. al.*[34] and Longo *et. al.*[40] respectively.

We have first obtained the electronic structures of R-VO$_2$ in the DFT and the DFT+U. In the DFT, stable metallic phases are obtained both in the nonmagnetic and the magnetic band structure calculation, in agreement with the experiment. However, in the DFT+U, more stable insulating phase is obtained in the magnetic band structure calculation,[41] which is seemingly in disagreement with the experiment. In fact, the insulating phase of R-VO$_2$ in the DFT+U had been reported before.[18, 19] This discrepancy can be resolved by considering the competition between the magnetic instability and the structural instability in R-VO$_2$. Of course, in nature, the structural instability wins over the magnetic instability, and so R-VO$_2$ undergoes the structural transition to M_1-VO$_2$ rather than the magnetic transition.

Figure 1 shows the phonon dispersion curves of R-VO$_2$ in the DFT and DFT+U. Four Raman modes (B$_{1g}$, E$_g$, A$_{1g}$, and B$_{2g}$) are obtained in both cases, in agreement with experiments.[29–31] The phonon softening instabilities are obtained both in the DFT (Fig. 1(a)) and in the DFT+U (Fig. 1(b)), which imply that R-VO$_2$ is not a stable structure. These results are expected because R-VO$_2$ is stable only at high temperature. The most noteworthy is the marked difference in the phonon dispersion curves between the DFT and the DFT+U. In the DFT, the phonon softenings occur at $\mathbf{q} = \Gamma$, M and X (Fig. 1(a)), while, in the DFT+U, they occur at $\mathbf{q} =$ R, A and Z (Fig. 1(b)). Indeed, the phonon softening at $\mathbf{q} =$ R was once predicted to be responsible for the transformation from R-VO$_2$ to M_1-VO$_2$.[32–36]

We have examined the normal modes of the softened phonons. The normal mode at $\mathbf{q} = \Gamma$ in the DFT is plotted in the inset of Fig. 1(a), and those at $\mathbf{q} =$ R in the DFT+U are plotted in Fig. 2(a) and (b). Recall that the main structural changes from R-VO$_2$ to M_1-VO$_2$ are the dimerization and zig-zag distortion of V ions, as shown in Fig. 2(d). It is evident that those lattice distortions cannot be described by the normal mode at Γ in the DFT. The softened modes at M and X in the DFT do not describe the structural distortions either. In contrast, the normal modes at R in the DFT+U are consistent with the lattice distortions of VO$_2$. As shown in Fig. 2(a) and (b), there are two degenerate softened phonon modes at R. The first mode in Fig. 2(a) represents the dimerizations of half of V ions and the orthogonal displacements of the other half. The second mode in Fig. 2(b) is just the reverse of the first one. Note that the mode predicted by Gervais *et al.*[36] is close to the first mode. Also similar modes to above two were once obtained by using a simple interatomic potential model.[42] A linearly superposed mode using these two normal modes in Fig. 2(c) reveals

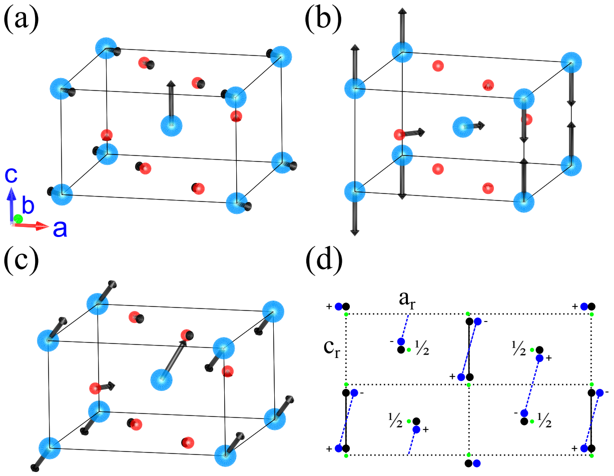

FIG. 2: (Color online) The normal modes of the softened phonons of R-VO$_2$ in the DFT+U at $\mathbf{q} =$ R. There are two degenerate modes, as shown in (a) and (b). (c) A linearly superposed mode at $\mathbf{q} =$ R using two degenerate modes of (a) and (b). The blue and red balls represent V and O, respectively. (d) Schematic picture of V-V pairing and distortion in M_1-VO$_2$. Blue, green, and black dots correspond to V ions in M$_1$-VO$_2$, R-VO$_2$, and M$_2$-VO$_2$), respectively.

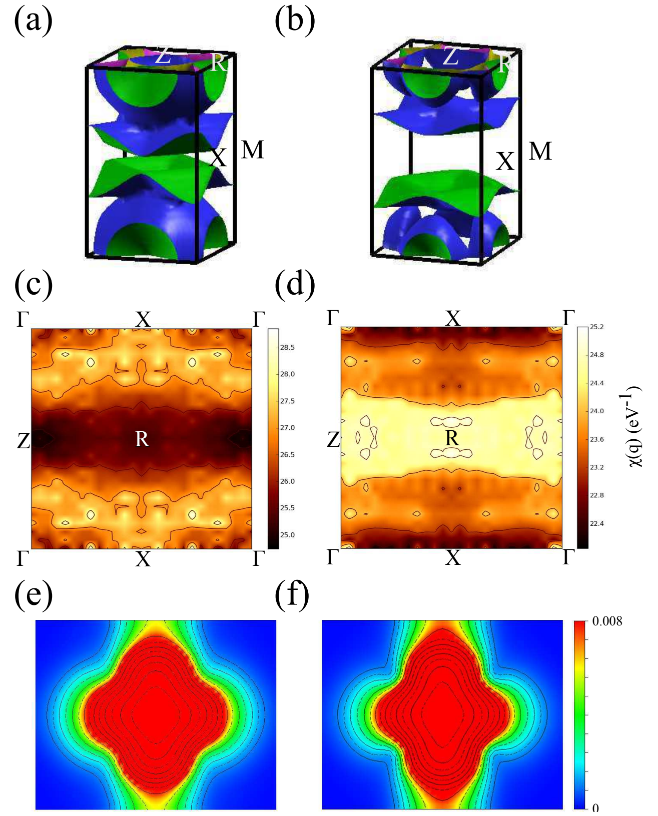

FIG. 3: (Color online) (a),(b) The Fermi surface of R-VO$_2$ in the DFT and in the DFT+U, respectively. (c),(d) $\chi(\mathbf{q})$ of R-VO$_2$ in the DFT and in the DFT+U, respectively. (e),(f) Local charge density near E_F around V ion (integrated over ~ -1.2 eV to E_F) in the DFT and in the DFT+U, respectively, in unit of (e/Å^3).

simultaneous dimerizations and zig-zag distortions of V ions, in good agreement with the observed lattice distortions in M_1-VO$_2$ (Fig. 2(d)). The other superposed mode also reveals similar displacements of V ions. This agreement demonstrates that the softened mode at R in the DFT+U describes the structural transition of VO$_2$ properly. The softened modes at A and Z in the DFT+U are also related to the dimerizations of V ions, but not directly to the zig-zag distortions of V ions.

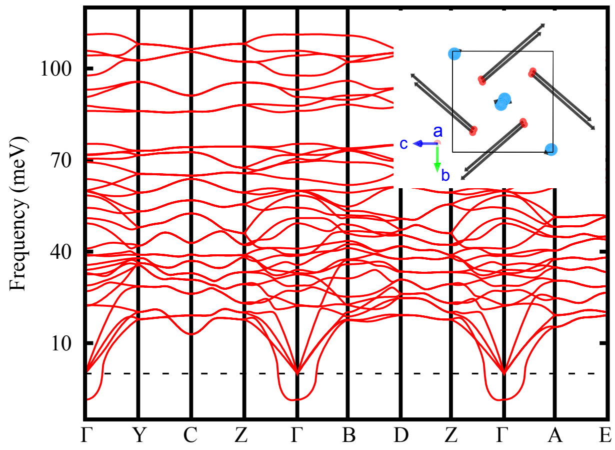

FIG. 4: (Color online) The phonon dispersion curve of M_1-VO$_2$ at the pressure of 35.1 GPa in the DFT. The inset shows the normal mode of the softened phonon at $\mathbf{q} = \Gamma$. The blue and red balls represent V and O, respectively.

The role of the Coulomb correlation effect in the structural transition in VO$_2$ has not been invoked as an essential factor before. The present phonon study clearly demonstrates that the Coulomb correlation in R-VO$_2$ facilitates the Peierls-type structural transition. Namely, in R-VO$_2$, the Coulomb correlation effect and the Peierls distortion are mutually cooperating in driving the MIT and the structural transition. To examine the U effect in more detail, we have checked the phonon dispersion curves with varying U. With increasing U, we have found that the softenings at $\mathbf{q} = \Gamma$, M and X disappear, whereas the softenings at $\mathbf{q}$ = A, R and Z emerge for $U \geq 4.0$ eV. This feature indicates that large enough U is required to produce the right Peierls distortions in VO$_2$.

Figure 3 shows the Fermi surface, the electric susceptibility $\chi(\mathbf{q})$, and the local charge density of R-VO$_2$ in the DFT and the DFT+U calculations. By comparing the Fermi surfaces in Fig. 3(a) and (b), one can notice that the Fermi surface becomes flatter in the DFT+U, suggesting a possible nesting effect along the c-axis.[43] This change is more apparent in $\chi(\mathbf{q})$. As compared to $\chi(\mathbf{q})$ in the DFT, $\chi(\mathbf{q})$ in the DFT+U exhibits high values at $\mathbf{q}$=(x,0,0.5) ($0 \leq x \leq 0.5$), which explains the origin of phonon softenings at $\mathbf{q}$=(x,0,0.5), that is, at Z and R in Fig. 1(b). Local charge density plots in Fig.3 (e) and (f) also support the proper description of the DFT+U for the structural transition of R-VO$_2$. As compared to the case of the DFT, the charge density in the DFT+U is seen to be more anisotropic, reflecting that more charges are accumulated in the bonding region along the c-axis. This phenomenon arises from the correlation-induced orbital redistribution, whereby a_{1g} state is more occupied than other e_g^π states. Accordingly, the system becomes more one dimensional-like along the c-axis, and so more susceptible to the Peierls transition.

Now we have investigated the stability of M_1-VO$_2$ under pressure. In the DFT calculation for M_1-VO$_2$, we have obtained the insulating phase at the ambient pressure, even though the energy gap is negligibly small ($\sim$ 0.03 eV). This result is different from existing DFT results, in which metallic phases were obtained for M_1-VO$_2$.[3–5] This difference is thought to come from the full relaxation of volume and ionic positions in our band calculations, which was not taken into account in the previous calculations. Without the relaxation, we also get the metallic phase for M_1-VO$_2$ in the DFT. In the DFT+U, we have obtained the insulating phase with energy gap of $\sim$ 0.67 eV, which agrees well with the experimental gap of 0.6-0.7 eV.[4, 44]

We have calculated the phonon dispersions of M_1-VO$_2$ both in the DFT and the DFT+U. In both cases, there are no phonon softening instabilities, which indicate that M_1-VO$_2$ is a stable structure at the ambient pressure. Interesting feature is obtained in the phonon dispersion of M_1-VO$_2$ under pressure. Figure 4 shows the phonon dispersion curve of M_1-VO$_2$ at 35.1 GPa in the DFT, which manifests the phonon softening instability at Γ. This softened mode implies that M_1-VO$_2$ would undergo a structural transition at some pressure $P \leq 35.1$ GPa. This result is indeed consistent with the experiments,[26–28] in which the pressure-induced transition from insulating M_1-VO$_2$ to a metallic phase of M_x-VO$_2$ was observed.

The normal mode of the softened phonon at Γ is depicted in the inset of Fig. 4, which shows the rotation of oxygen (O) octahedron with slight displacements of V ions. The transformation from M_1-VO$_2$ to M_x-VO$_2$ is expected to arise from this rotation mode. In the experiment under pressure, the anisotropic compression was observed in M_x-VO$_2$.[28] Lattice constants b and c become softened and hardened, respectively, while a decreases regularly. This anisotropy is reminiscent of the case of CrO$_2$, which also has a pressure-induced structural transition from rutile to CaCl$_2$-type with the softened normal mode of the O octahedron rotation. Anisotropic compression is also present in CrO$_2$ of CaCl$_2$-type.[45, 46] This similarity suggests that M_x-VO$_2$ would have a monoclinic structure of CaCl$_2$-type.

In conclusion, based on the phonon dispersion studies in the DFT and the DFT+U, we have demonstrated that the driving mechanism of the MIT and the structural transition in VO$_2$ is the Mott-Peierls transition. The Coulomb correlation effect in R-VO$_2$ plays an essential role of assisting the Peierls transition. The softened phonon mode at $\mathbf{q} = \mathrm{R}$ in the DFT+U describes properly the structural transition from R-VO$_2$ to M_1-VO$_2$. Further, we have found that M_1-VO$_2$ becomes unstable under high pressure due to the phonon softening at Γ. This softened mode is expected to have the relation to the pressure-induced transition from M_1-VO$_2$ to M_x-VO$_2$, which is predicted to have a monoclinic structure of CaCl$_2$-type.

This work was supported by the NRF (No. 2009-0079947, No. 2011-0025237) and the KISTI supercomputing center (No. KSC-2012-C2-18). S.K. acknowledges the support from the NRF project of Global Ph.D. Fellowship (No. 2011-0002351).

[1] F. J. Morin, Phys. Rev. Lett. **3** 34 (1959).

[2] J. Goodenough, Phys. Rev. **117**, 1442 (1960).

[3] V. Eyert, Ann. Phys. (Leipzig) **11**, 650 (2002).

[4] R. M. Wentzcovitch, W. W. Schulz, and P. B. Allen, Phys. Rev. Lett. **72**, 3389 (1994)

[5] A. Liebsch, H. Ishida, and G. Bihlmayer, Phys. Rev. B **71**, 085109 (2005).

[6] A. Zylbersztejn and N. F. Mott, Phys. Rev. B **11** 4393 (1975).

[7] T. M. Rice, H. Launois, and J. P. Pouget, Phys. Rev. Lett. **73** 3042 (1994).

[8] H.-T. Kim, Yong Wook Lee, Bong-Jun Kim, Byung-Gyu Chae, Sun Jin Yun, Kwang-Yong Kang, Kang-Jeon Han, Ki-Ju Yee, and Yong-Sik Lim, Phys. Rev. Lett. **97**, 266401 (2006).

[9] A. Continenza, S. Massidda, and M. Posternak, Phys. Rev. B **60**, 15699 (1999).

[10] M. Gatti, F. Bruneval, V. Olevano, and L. Reining, Phys. Rev. Lett. **99**, 266402 (2007).

[11] R. Sakuma, T. Miyake, and F. Aryasetiawan, Phys. Rev. B **78**, 075106 (2008).

[12] V. Eyert, Phys. Rev. Lett. **107**, 016401 (2011).

[13] S. Biermann, A. Poteryaev, A. I. Lichtenstein, and A. Georges, Phys. Rev. Lett. **94** 026404 (2005).

[14] B. Lazarovits, K. Kim, K. Haule, and G. Kotliar, Phys. Rev. B **81**, 115117 (2010).

[15] A. S. Belozerov, M. A. Korotin, V. I. Anisimov, and A. I. Poteryaev, Phys. Rev. B **85**, 045109 (2012).

[16] M. W. Haverkort, Z. Hu, A. Tanaka, W. Reichelt, S. V. Streltsov, M. A. Korotin, V. I. Anisimov, H. H. Hsieh, H.-J. Lin, C. T. Chen, D. I. Khomskii, and L. H. Tjeng, Phys. Rev. Lett. **95**, 196404 (2005).

[17] C. Weber, D. D. Ø'Regan, N. D. M. Hine, M. C. Payne, G. Kotliar, and Peter B. Littlewood, Phys. Rev. Lett. 108, 256402 (2012).

[18] M. A. Korotin, N. A. Shorikov, and V. I. Anisimov, Phys. Met. Metallogr. **94**, 17 (2002)

[19] G.-H. Liu, X.-Y. Deng, and R. Wen, J. Mater. Sci. **45**, 3270 (2010).

[20] A. S. Belozerov, A. I. Poteryaev, and V. I. Anisimov, JETP Lett. **93**, 73 (2011).

[21] M. Marezio, D. B. McWhan, J. P. Remeika, and P. D. Dernier, Phys. Rev. B **5** 2541 (1972).

[22] J. P. Pouget, H. Launois, T. M. Rice, P. Dernier, A. Gossard, G. Villeneuve, and P. Hagenmuller, Phys. Rev. B **10**, 1801 (1974).

[23] J. P. Pouget, H. Launois, J. P. D'Haenens, P. Merenda, and T.M. Rice, Phys. Rev. Lett. **35**, 873 (1975).

[24] M. Ghedira, J. Chenavas, and M. Marezio, J. Phys. C **10** L309 (1977).

[25] M. Ghedira, H. Vincent, M. Marezio, and J. C. Launay, J. Solid State Chem. **22** 423 (1977).

[26] E. Arcangeletti, L. Baldassarre, D. Di Castro, S. Lupi, L. Malavasi, C. Marini, A. Perucchi, and P. Postorino, Phys. Rev. Lett. **98**, 196406 (2007).

[27] C. Marini, E. Arcangeletti, D. Di Castro, L. Baldassare, A. Perucchi, S. Lupi, L. Malavasi, L. Boeri, E. Pomjakushina, K. Conder, and P. Postorino, Phys. Rev. B **77**, 235111 (2008).

[28] M. Mitrano, B. Maroni, C. Marini, M. Hanfland, B. Joseph, P. Postorino, and L. Malavasi, Phys. Rev. B **85**, 184108 (2012).

[29] R. Srivastava and L. Chase, Phys. Rev. Lett. **27**, 727 (1971).

[30] P. Schilbe, Physica B: Cond. Matt. **316-317**, 600-602

(2002).

[31] P. Schilbe and D. Maurer, Mat. Scie. and Engin.: A **370**, 449 (2004).

[32] J. R. Brews, Phys. Rev. B **1**, 2557 (1970).

[33] C. J. Hearnt, J. Phys. C: Solid State Phys. **5**, 1317 (1972).

[34] D. B. McWhan, M. Marezio, J. P. Remeika, and P. D. Dernier, Phys. Rev. B **10**, 490 (1974).

[35] H. Terauchi and J. B. Cohen, Phys. Rev. B **17**, 2494 (1978).

[36] F. Gervais and W. Kress, Phys. Rev. B **31**, 4809 (1985).

[37] G. Kresse and J. Furthmüller, Phys. Rev. B **54**, 11169 (1996); Comput. Mater. Sci. **6**, 15 (1996).

[38] A. Togo, F. Oba, and I. Tanaka, Phys. Rev. B. **78**, 134106 (2008).

[39] The selected **k**-point samplings are (6×6×10) for R-VO$_2$, (6×8×6) for M_1-VO$_2$ in the Monkhorst-Pack grid.

[40] J.M. Longo and P. Kierkegaard, Acta Chem. Scand. **24**, 420 (1970).

[41] The energy gaps and the magnetizations were obtained to be 0.86 eV and $\sim 1.1\mu_B$ for the ferromagnetic case, while 1.25 eV and $\sim 1.1\mu_B$ for the antiferromagnetic case.

[42] S. M. Woodley, Chem. Phys. Lett. **453**, 167 (2008).

[43] M. Gupta, A. J. Freeman, and D. E. Ellis, Phys. Rev. B **16**, 3338 (1977)

[44] S. Shin, S. Suga, M. Taniguchi, M. Fujisawa, H. Kanzaki, A. Fujimori, H. Daimon, Y. Ueda, K. Kosuge, and S. Kachi, Phys. Rev. B **41**, 4993 (1990).

[45] B. R. Maddox, C. S. Yoo, D. Kasinathan, W. E. Pickett, and R. T. Scalettar, Phys. Rev. B **73**, 144111 (2006).

[46] S. Kim, K. Kim, C.-J. Kang, and B. I. Min, Phys. Rev. B **85**, 094106 (2012).